Cell Reports, Volume *42*

Supplemental information

Lateral entorhinal cortex inputs modulate hippocampal dendritic excitability by recruiting a local disinhibitory microcircuit

Olesia M. Bilash, Spyridon Chavlis, Cara D. Johnson, Panayiota Poirazi, and Jayeeta Basu

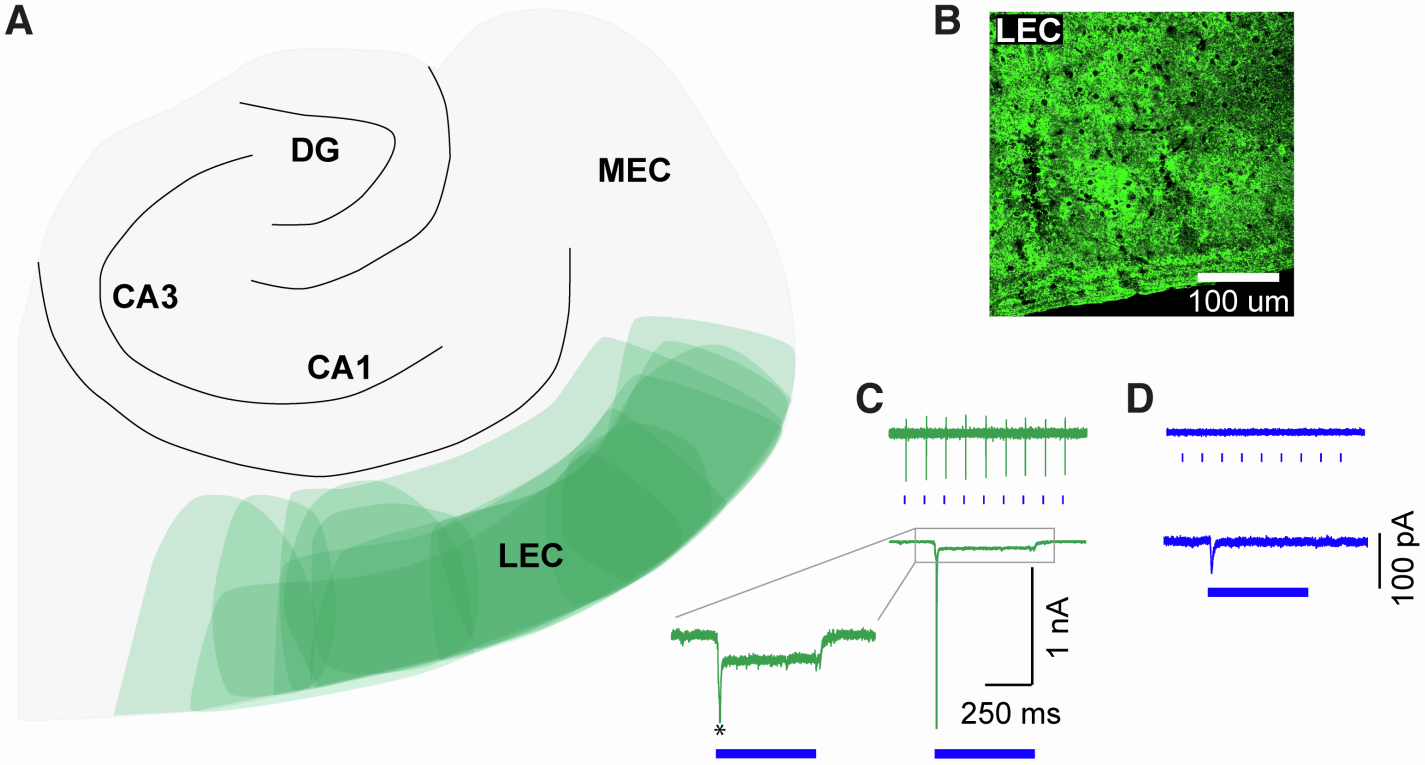
A
DG
MEC
CA3
CA1
LEC
B
LEC
100 um
C
1 nA
250 ms
D
100 pA

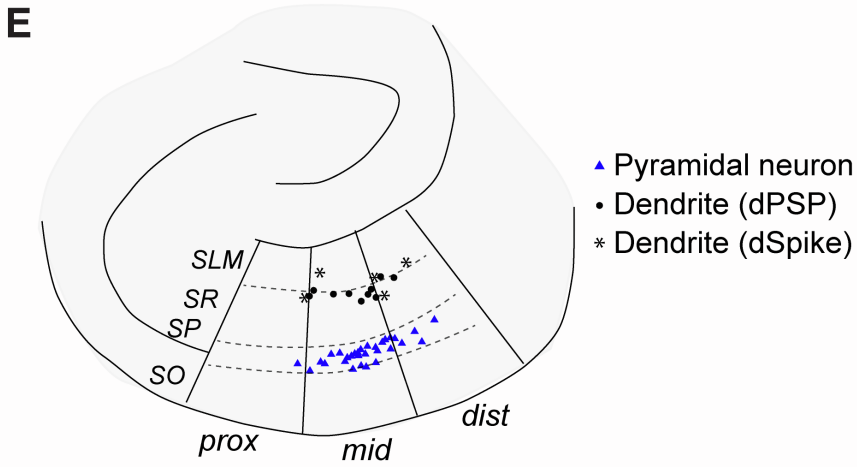
E
SLM
SR
SP
SO
prox
mid
dist
Pyramidal neuron
Dendrite (dPSP)
Dendrite (dSpike)

Figure S1

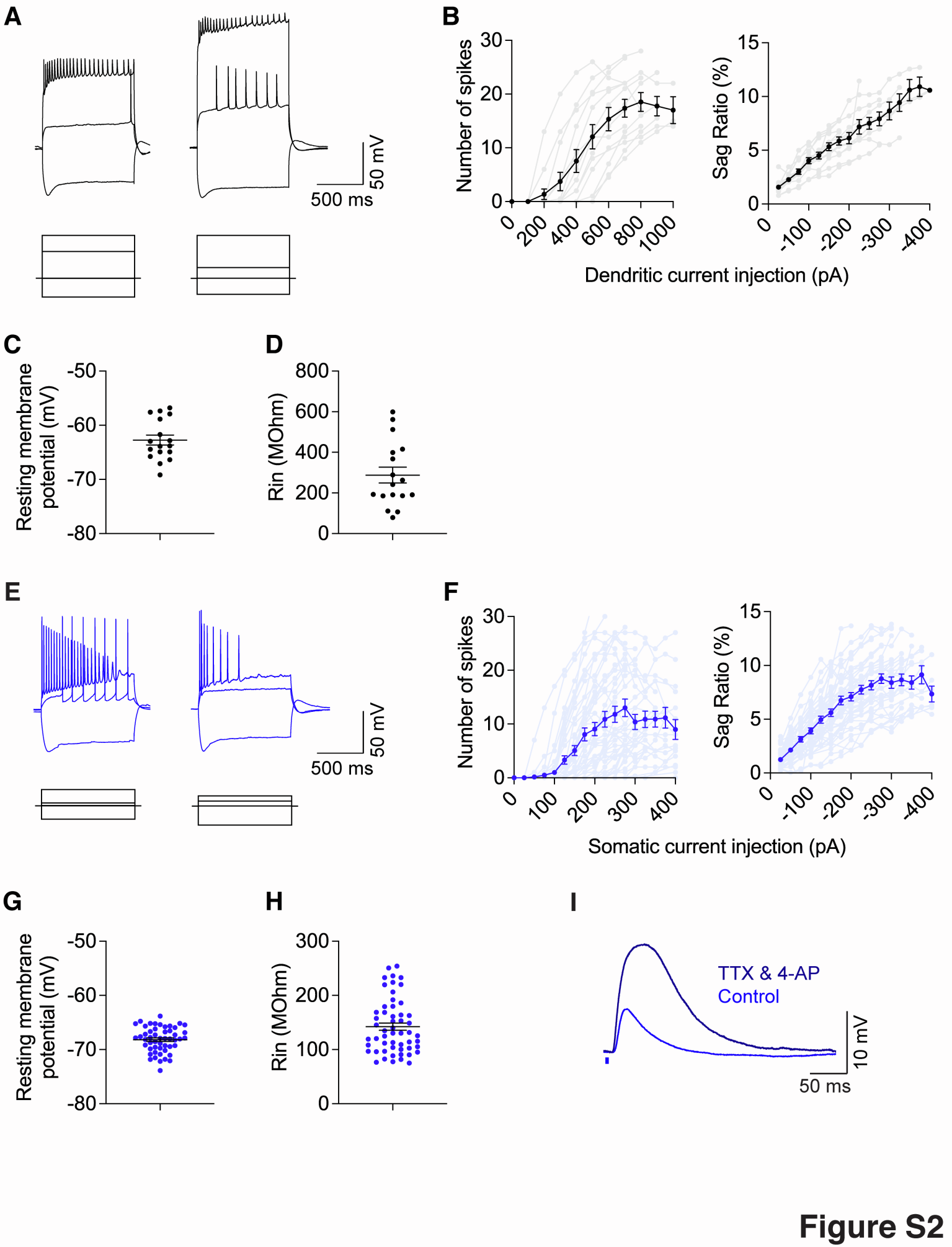
A
50 mV
500 ms
B
Number of spikes
Sag Ratio (%)
Dendritic current injection (pA)
C
Resting membrane potential (mV)
D
Rin (MOhm)
E
50 mV
500 ms
F
Number of spikes
Sag Ratio (%)
Somatic current injection (pA)
G
Resting membrane potential (mV)
H
Rin (MOhm)
I
TTX & 4-AP
Control
10 mV
50 ms

Figure S2

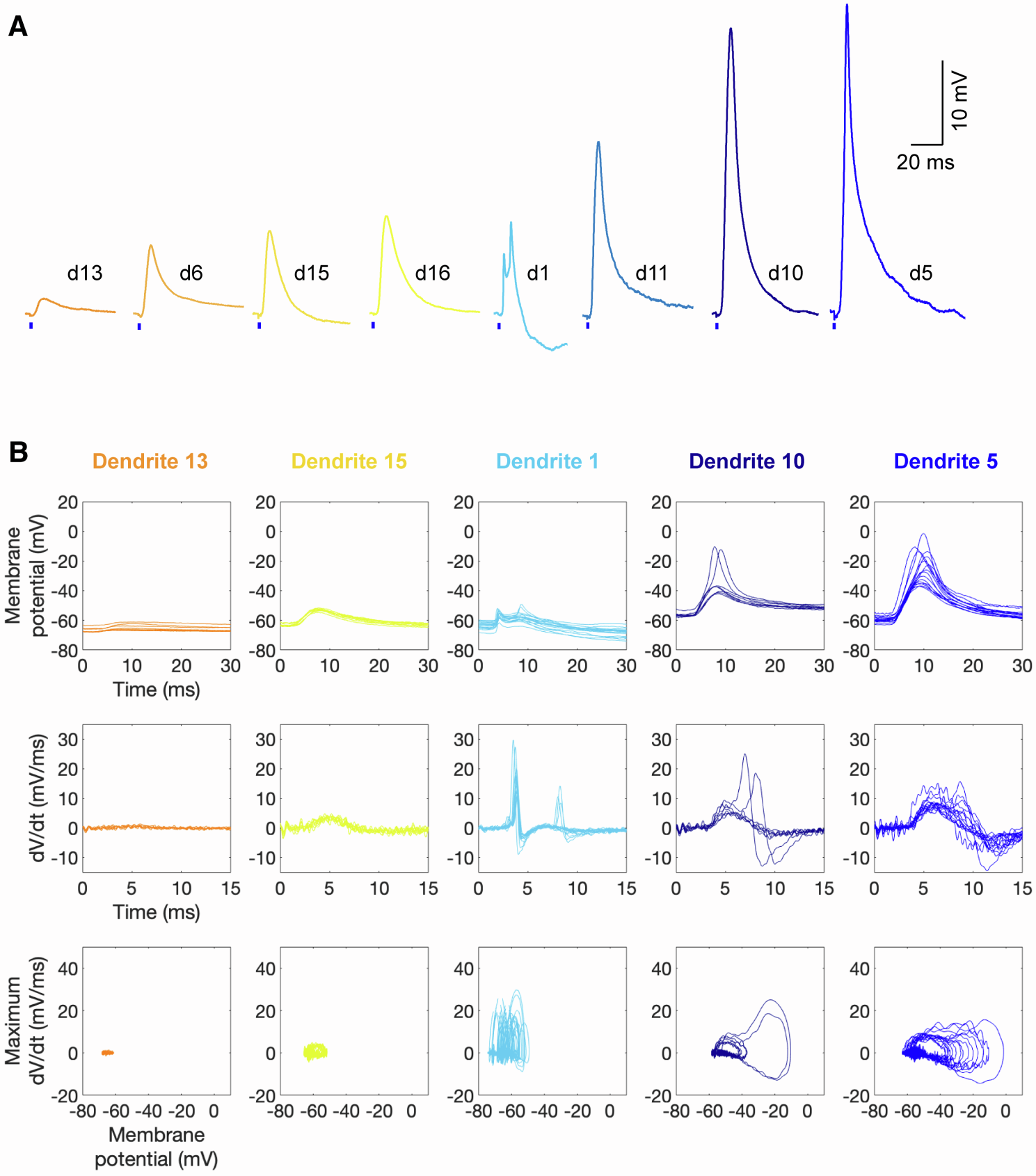
A
d13
d6
d15
d16
d1
d11
d10
d5
10 mV
20 ms
B
Dendrite 13
Dendrite 15
Dendrite 1
Dendrite 10
Dendrite 5
Membrane potential (mV)
Time (ms)
dV/dt (mV/ms)
Time (ms)
Maximum dV/dt (mV/ms)
Membrane potential (mV)

Figure S3

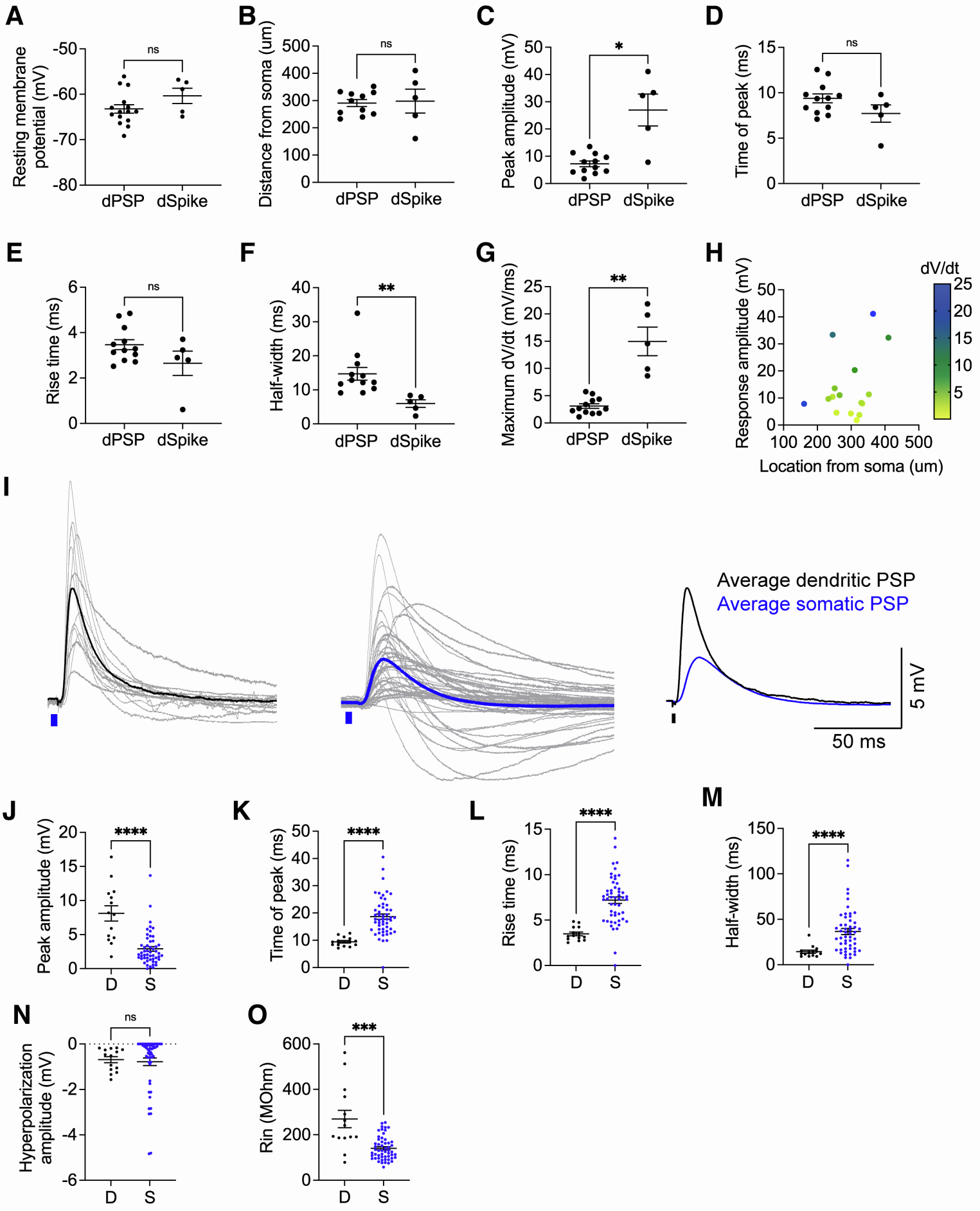
A
Resting membrane potential (mV)
-50
-60
-70
-80
ns
dPSP
dSpike
B
Distance from soma (um)
500
400
300
200
100
0
ns
dPSP
dSpike
C
Peak amplitude (mV)
50
40
30
20
10
0
*
dPSP
dSpike
D
Time of peak (ms)
15
10
5
0
ns
dPSP
dSpike
E
Rise time (ms)
6
4
2
0
ns
dPSP
dSpike
F
Half-width (ms)
40
30
20
10
0
**
dPSP
dSpike
G
Maximum dV/dt (mV/ms)
25
20
15
10
5
0
**
dPSP
dSpike
H
Response amplitude (mV)
50
40
30
20
10
0
100 200 300 400 500
Location from soma (um)
dV/dt
25
20
15
10
5
I
Average dendritic PSP
Average somatic PSP
5 mV
50 ms
J
Peak amplitude (mV)
20
15
10
5
0
****
D
S
K
Time of peak (ms)
50
40
30
20
10
0
****
D
S
L
Rise time (ms)
15
10
5
0
****
D
S
M
Half-width (ms)
150
100
50
0
****
D
S
N
Hyperpolarization amplitude (mV)
0
-2
-4
-6
ns
D
S
O
Rin (MOhm)
600
400
200
0
***
D
S

Figure S4

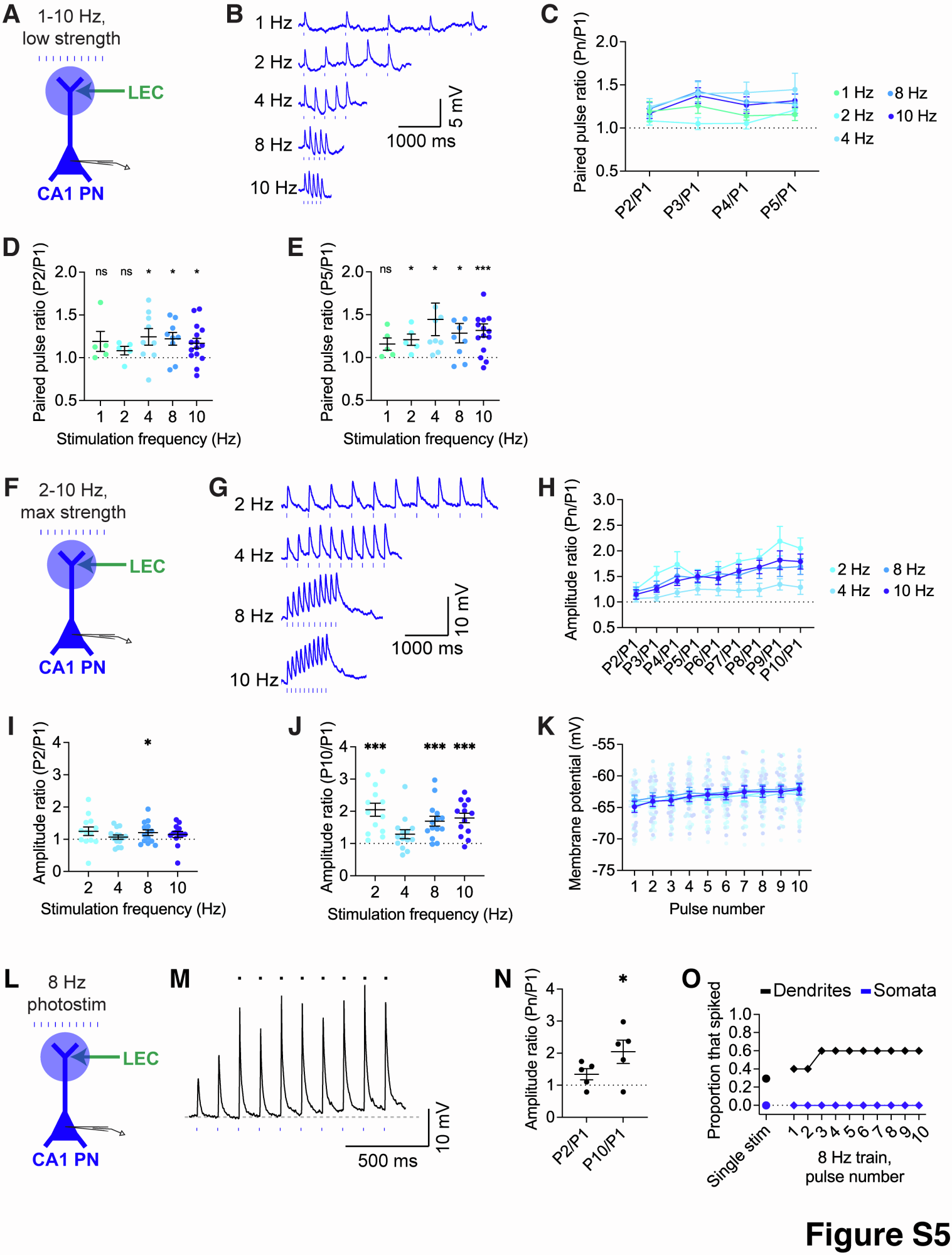
A
1-10 Hz,
low strength
LEC
CA1 PN
B
1 Hz
2 Hz
4 Hz
8 Hz
10 Hz
5 mV
1000 ms
C
Paired pulse ratio (Pn/P1)
2.0
1.5
1.0
0.5
P2/P1
P3/P1
P4/P1
P5/P1
1 Hz
2 Hz
4 Hz
8 Hz
10 Hz
D
Paired pulse ratio (P2/P1)
ns ns * * *
1 2 4 8 10
Stimulation frequency (Hz)
E
Paired pulse ratio (P5/P1)
ns * * * ***
1 2 4 8 10
Stimulation frequency (Hz)
F
2-10 Hz,
max strength
LEC
CA1 PN
G
2 Hz
4 Hz
8 Hz
10 Hz
10 mV
1000 ms
H
Amplitude ratio (Pn/P1)
3.0
2.5
2.0
1.5
1.0
0.5
P2/P1
P3/P1
P4/P1
P5/P1
P6/P1
P7/P1
P8/P1
P9/P1
P10/P1
2 Hz
4 Hz
8 Hz
10 Hz
I
Amplitude ratio (P2/P1)
*
2 4 8 10
Stimulation frequency (Hz)
J
Amplitude ratio (P10/P1)
*** *** ***
2 4 8 10
Stimulation frequency (Hz)
K
Membrane potential (mV)
-55
-60
-65
-70
-75
1 2 3 4 5 6 7 8 9 10
Pulse number
L
8 Hz
photostim
LEC
CA1 PN
M
10 mV
500 ms
N
Amplitude ratio (Pn/P1)
*
P2/P1
P10/P1
O
Dendrites
Somata
Proportion that spiked
1.0
0.8
0.6
0.4
0.2
0.0
Single stim
1 2 3 4 5 6 7 8 9 10
8 Hz train,
pulse number

Figure S5

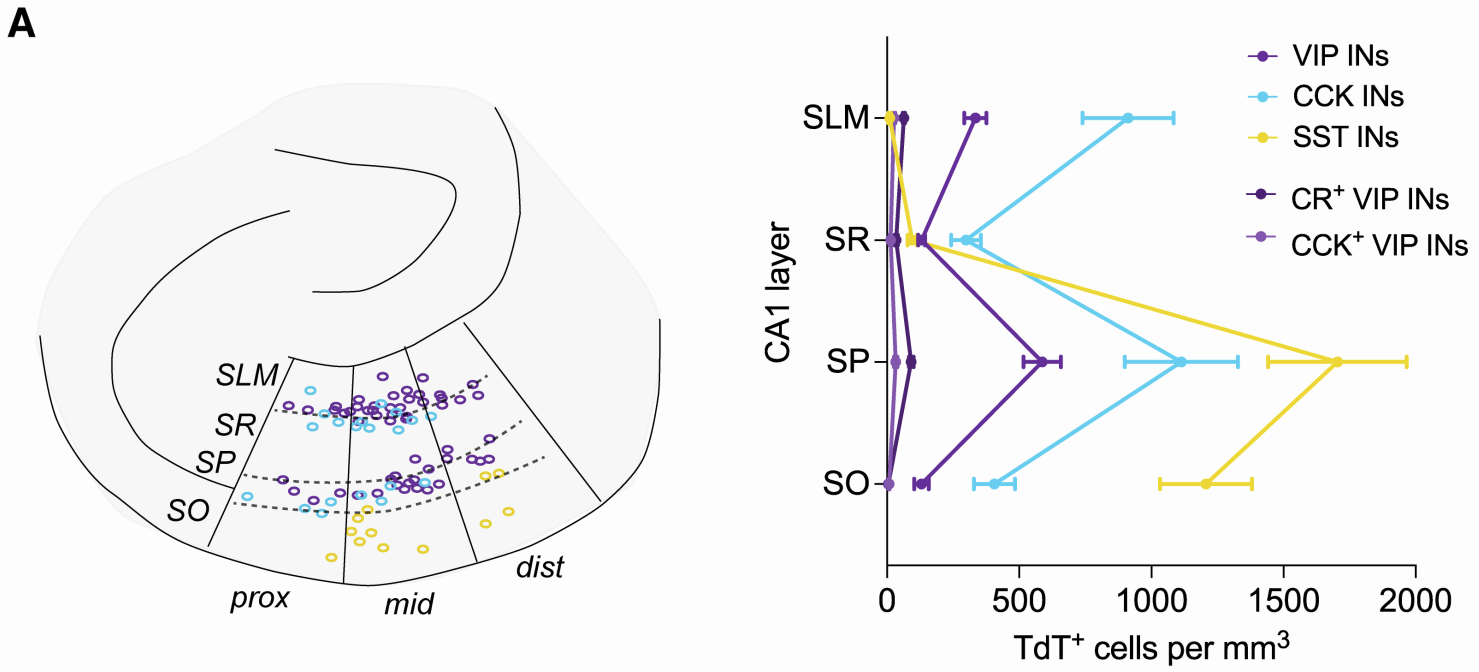
A
SLM
SR
SP
SO
prox
mid
dist
VIP INs
CCK INs
SST INs
CR+ VIP INs
CCK+ VIP INs
CA1 layer
SLM
SR
SP
SO
0
500
1000
1500
2000
TdT+ cells per mm3

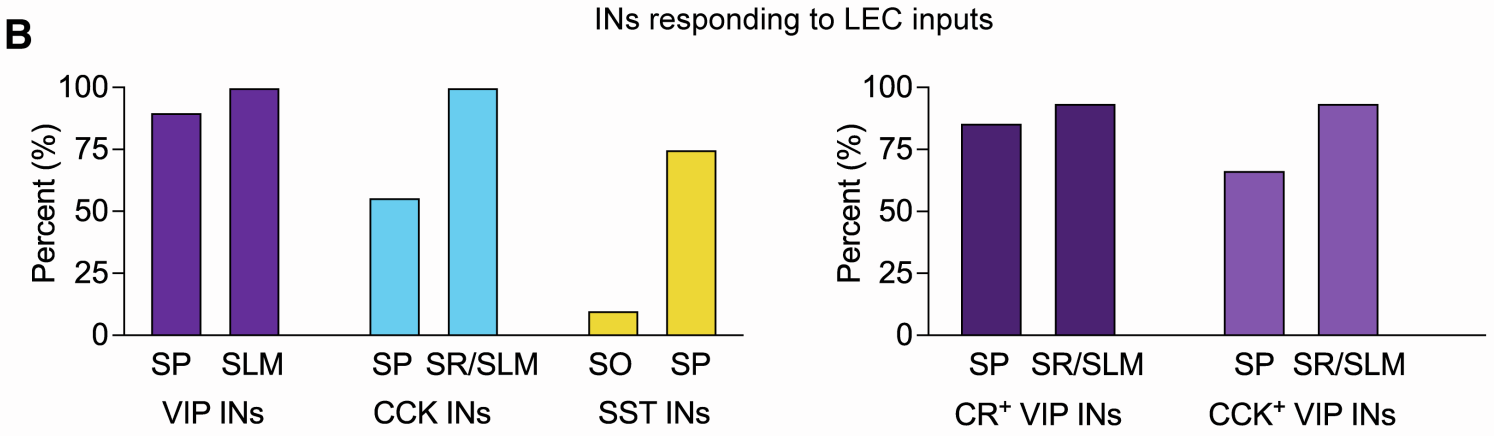
B
INs responding to LEC inputs
Percent (%)
100
75
50
25
0
SP
SLM
SP
SR/SLM
SO
SP
VIP INs
CCK INs
SST INs
SP
SR/SLM
SP
SR/SLM
CR+ VIP INs
CCK+ VIP INs

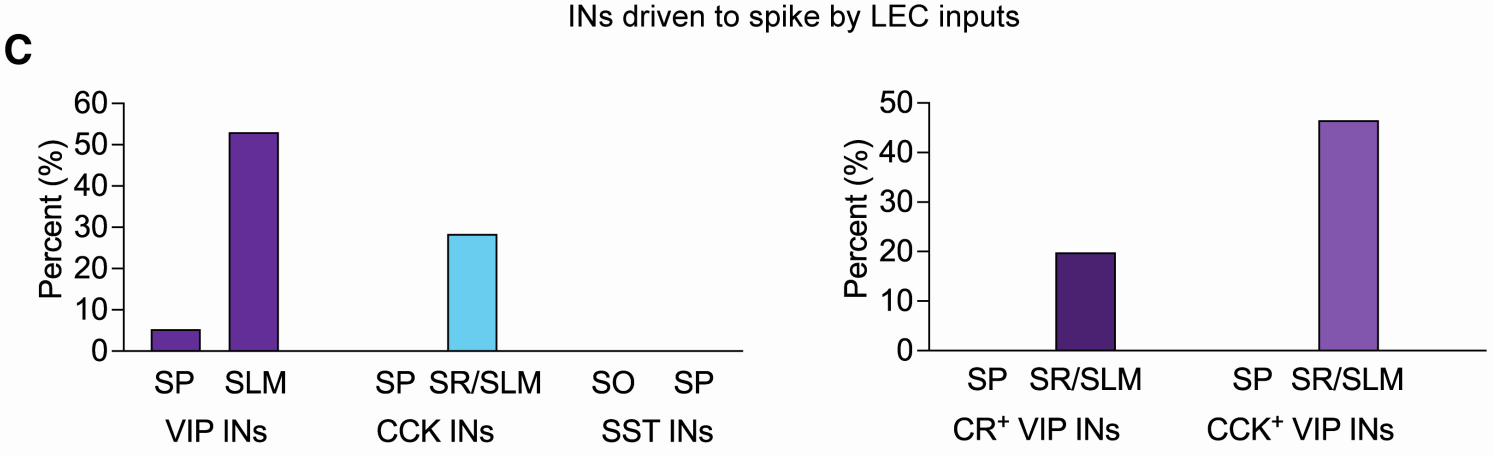
C
INs driven to spike by LEC inputs
Percent (%)
60
50
40
30
20
10
0
SP
SLM
SP
SR/SLM
SO
SP
VIP INs
CCK INs
SST INs
50
40
30
20
10
0
SP
SR/SLM
SP
SR/SLM
CR+ VIP INs
CCK+ VIP INs

Figure S6

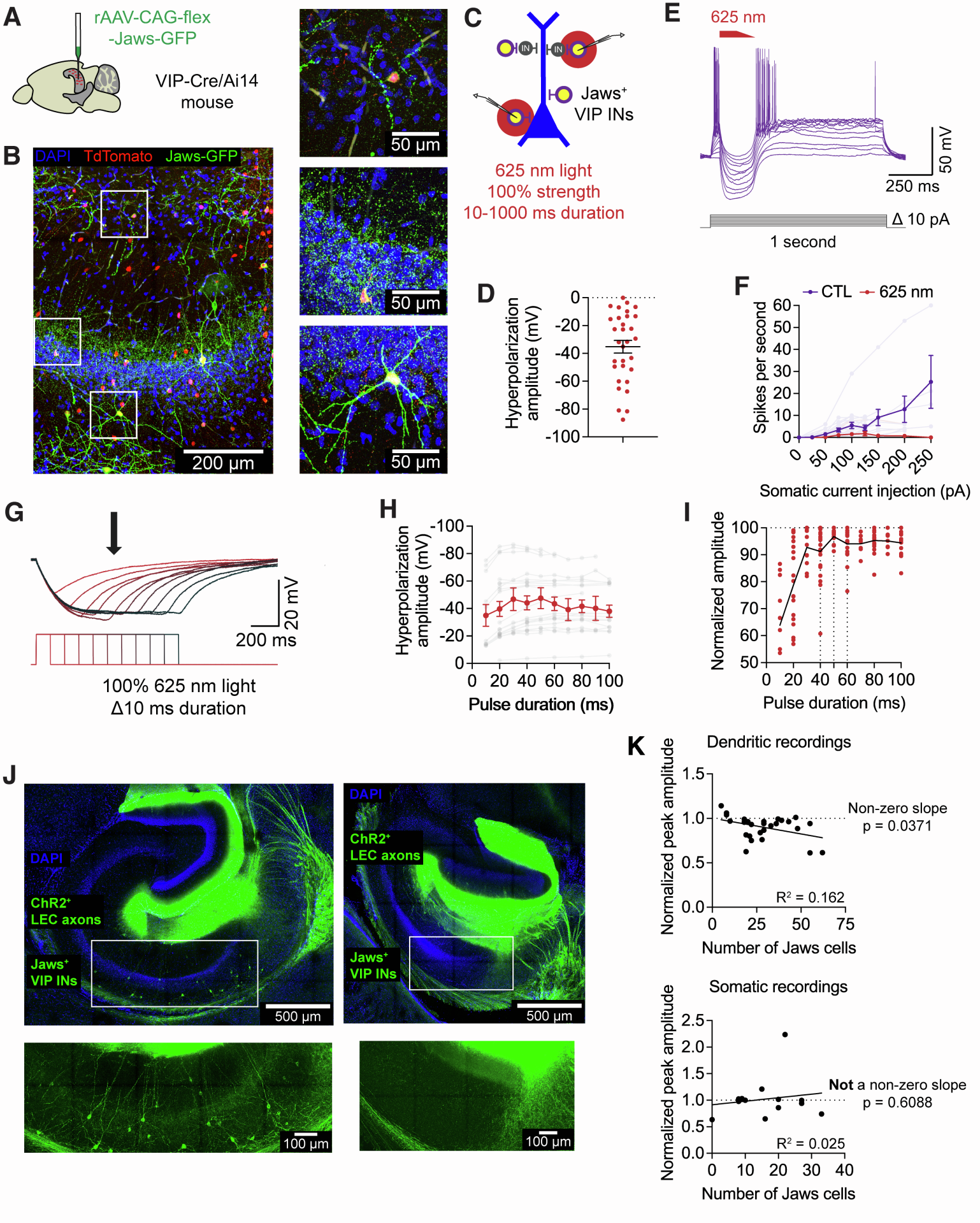
A
rAAV-CAG-flex
-Jaws-GFP
VIP-Cre/Ai14
mouse
B
DAPI TdTomato Jaws-GFP
200 µm
50 µm
50 µm
50 µm
C
IN
IN
Jaws+
VIP INs
625 nm light
100% strength
10-1000 ms duration
D
Hyperpolarization
amplitude (mV)
0
-20
-40
-60
-80
-100
E
625 nm
50 mV
250 ms
Δ 10 pA
1 second
F
CTL
625 nm
Spikes per second
60
50
40
30
20
10
0
0
50
100
150
200
250
Somatic current injection (pA)
G
20 mV
200 ms
100% 625 nm light
Δ10 ms duration
H
Hyperpolarization
amplitude (mV)
-100
-80
-60
-40
-20
0
0 20 40 60 80 100
Pulse duration (ms)
I
Normalized amplitude
100
90
80
70
60
50
0 20 40 60 80 100
Pulse duration (ms)
J
DAPI
ChR2+
LEC axons
Jaws+
VIP INs
500 µm
DAPI
ChR2+
LEC axons
Jaws+
VIP INs
500 µm
100 µm
100 µm
K
Dendritic recordings
Normalized peak amplitude
1.5
1.0
0.5
0.0
Non-zero slope
p = 0.0371
R² = 0.162
0
25
50
75
Number of Jaws cells
Somatic recordings
Normalized peak amplitude
2.5
2.0
1.5
1.0
0.5
0.0
Not a non-zero slope
p = 0.6088
R² = 0.025
0
10
20
30
40
Number of Jaws cells

Figure S7

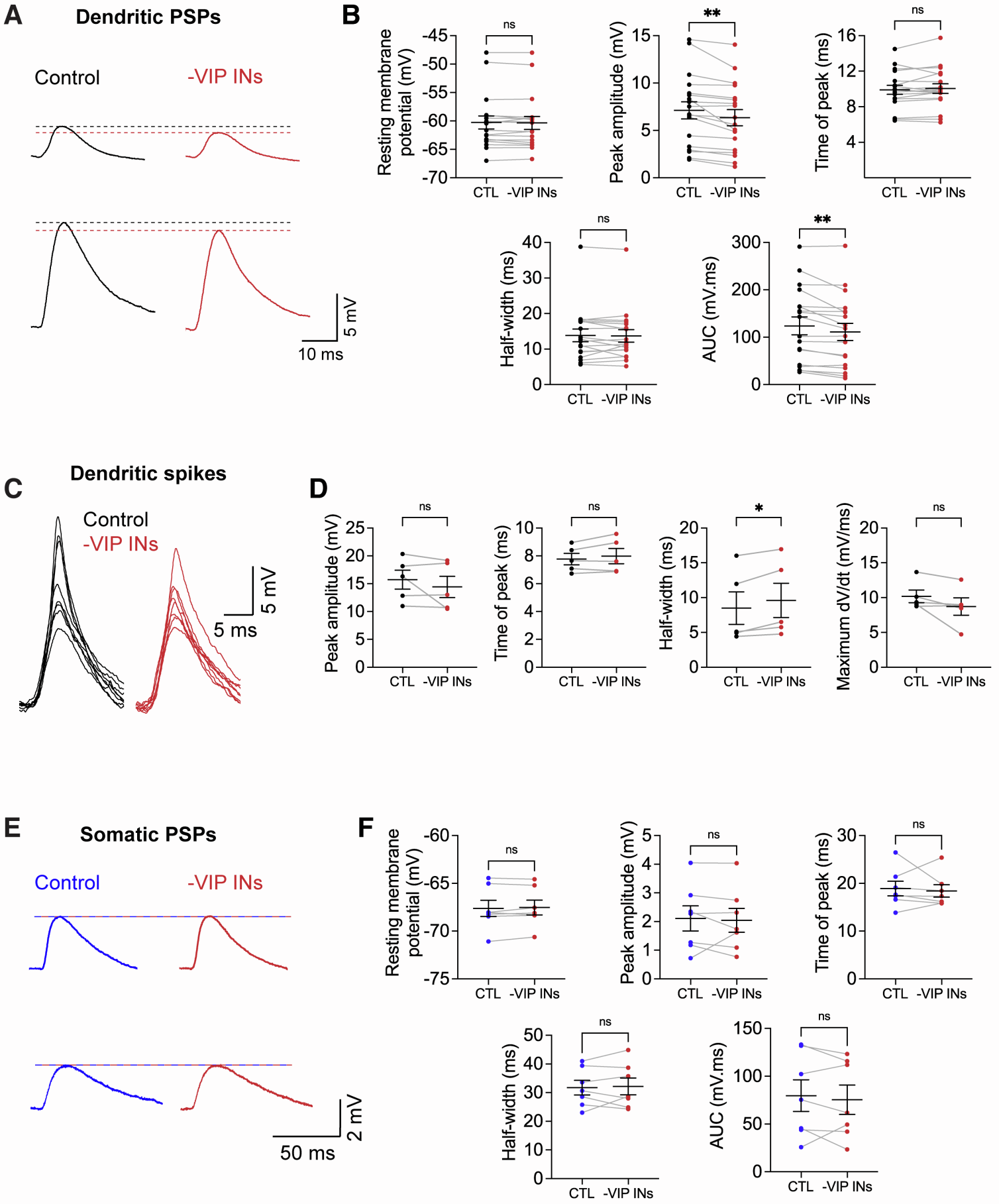
A
Dendritic PSPs
Control
-VIP INs
5 mV
10 ms
B
Resting membrane potential (mV)
Peak amplitude (mV)
Time of peak (ms)
Half-width (ms)
AUC (mV.ms)
ns
**
CTL -VIP INs
C
Dendritic spikes
Control
-VIP INs
5 mV
5 ms
D
Peak amplitude (mV)
Time of peak (ms)
Half-width (ms)
Maximum dV/dt (mV/ms)
ns
*
CTL -VIP INs
E
Somatic PSPs
Control
-VIP INs
2 mV
50 ms
F
Resting membrane potential (mV)
Peak amplitude (mV)
Time of peak (ms)
Half-width (ms)
AUC (mV.ms)
ns
CTL -VIP INs

Figure S8

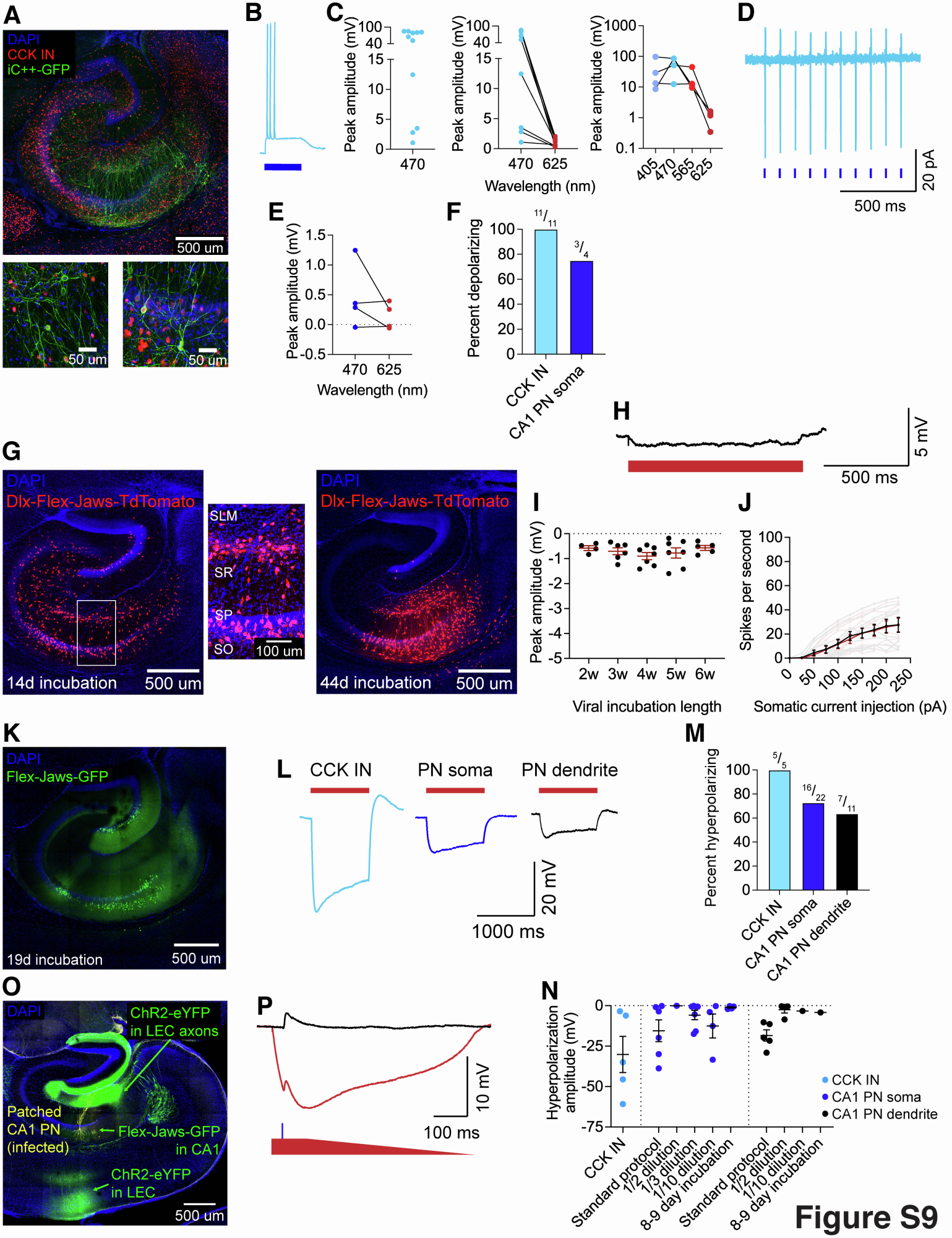
A
DAPI
CCK IN
iC++-GFP
500 um
50 um
50 um
B
C
Peak amplitude (mV)
100
40
15
10
5
0
470
Peak amplitude (mV)
100
40
15
10
5
0
470 625
Wavelength (nm)
Peak amplitude (mV)
1000
100
10
1
0.1
405 470 565 625
D
20 pA
500 ms
E
Peak amplitude (mV)
1.5
1.0
0.5
0.0
-0.5
470 625
Wavelength (nm)
F
Percent depolarizing
100
80
60
40
20
0
11/11
3/4
CCK IN
CA1 PN soma
H
5 mV
500 ms
G
DAPI
Dlx-Flex-Jaws-TdTomato
14d incubation
500 um
SLM
SR
SP
SO
100 um
DAPI
Dlx-Flex-Jaws-TdTomato
44d incubation
500 um
I
Peak amplitude (mV)
0
-1
-2
-3
-4
-5
2w 3w 4w 5w 6w
Viral incubation length
J
Spikes per second
100
80
60
40
20
0
0 50 100 150 200 250
Somatic current injection (pA)
K
DAPI
Flex-Jaws-GFP
19d incubation
500 um
L
CCK IN
PN soma
PN dendrite
20 mV
1000 ms
M
Percent hyperpolarizing
100
80
60
40
20
0
5/5
16/22
7/11
CCK IN
CA1 PN soma
CA1 PN dendrite
O
DAPI
ChR2-eYFP
in LEC axons
Patched
CA1 PN
(infected)
Flex-Jaws-GFP
in CA1
ChR2-eYFP
in LEC
500 um
P
10 mV
100 ms
N
Hyperpolarization
amplitude (mV)
0
-25
-50
-75
CCK IN
Standard protocol
1/2 dilution
1/3 dilution
1/10 dilution
8-9 day incubation
Standard protocol
1/2 dilution
1/10 dilution
8-9 day incubation
CCK IN
CA1 PN soma
CA1 PN dendrite

Figure S9

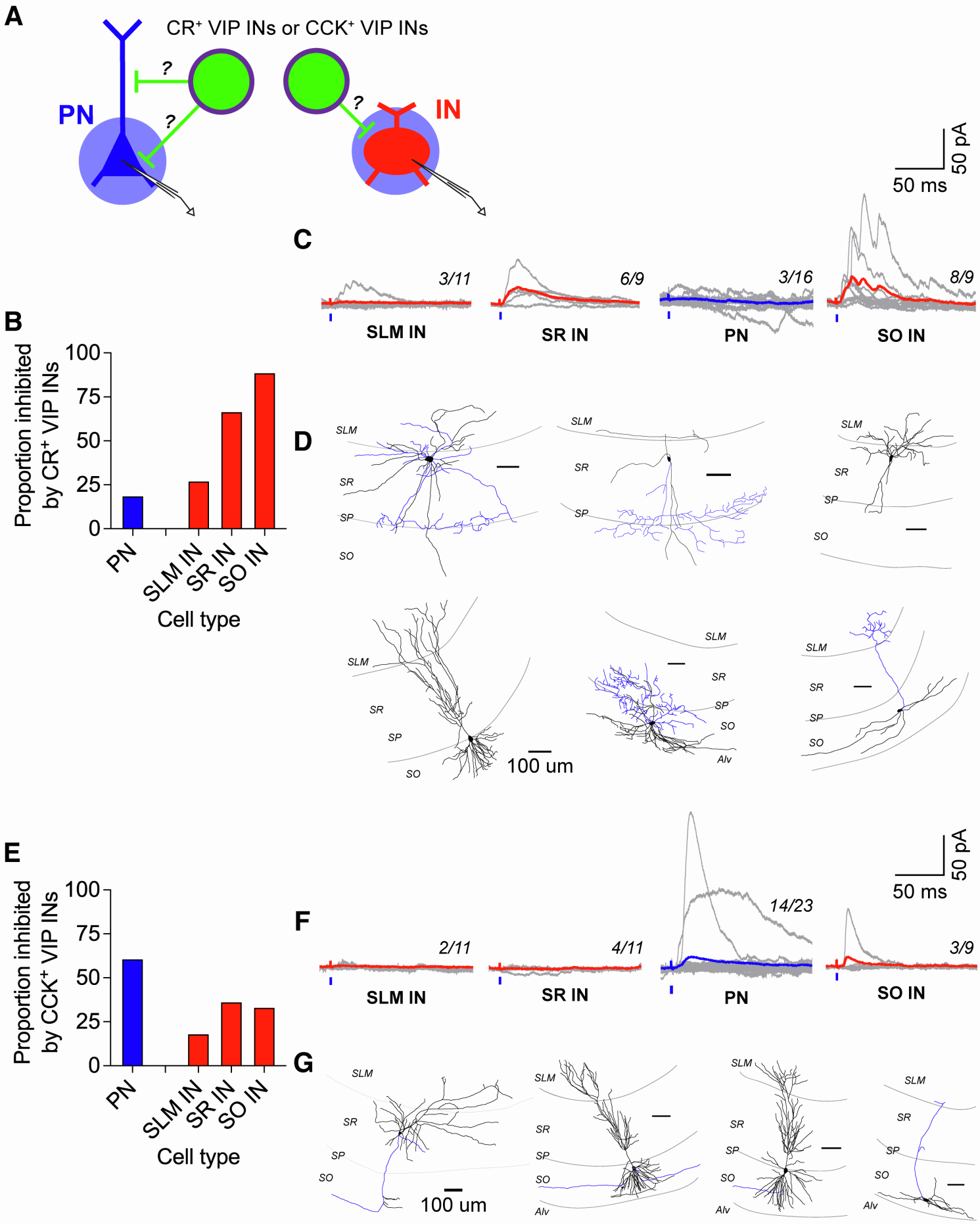
A
CR+ VIP INs or CCK+ VIP INs
PN
IN
?
?
?
50 pA
50 ms
C
3/11
6/9
3/16
8/9
SLM IN
SR IN
PN
SO IN
B
Proportion inhibited by CR+ VIP INs
100
75
50
25
0
PN
SLM IN
SR IN
SO IN
Cell type
D
SLM
SR
SP
SO
Alv
100 um
E
Proportion inhibited by CCK+ VIP INs
100
75
50
25
0
PN
SLM IN
SR IN
SO IN
Cell type
F
50 pA
50 ms
2/11
4/11
14/23
3/9
SLM IN
SR IN
PN
SO IN
G
SLM
SR
SP
SO
Alv
100 um

Figure S10

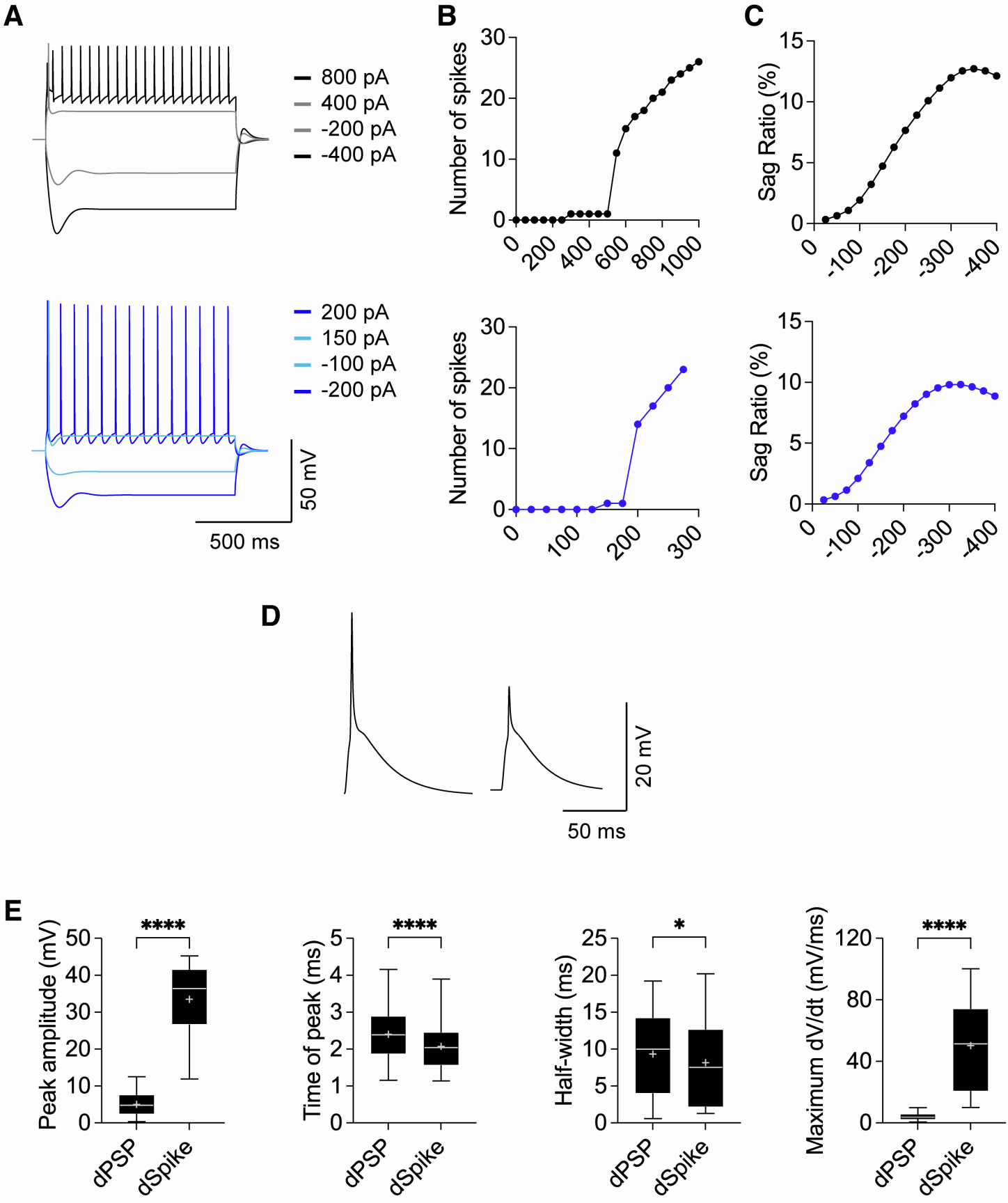
A
800 pA
400 pA
-200 pA
-400 pA
200 pA
150 pA
-100 pA
-200 pA
50 mV
500 ms
B
Number of spikes
C
Sag Ratio (%)
D
20 mV
50 ms
E
Peak amplitude (mV)
Time of peak (ms)
Half-width (ms)
Maximum dV/dt (mV/ms)
****
*
dPSP
dSpike

Figure S11

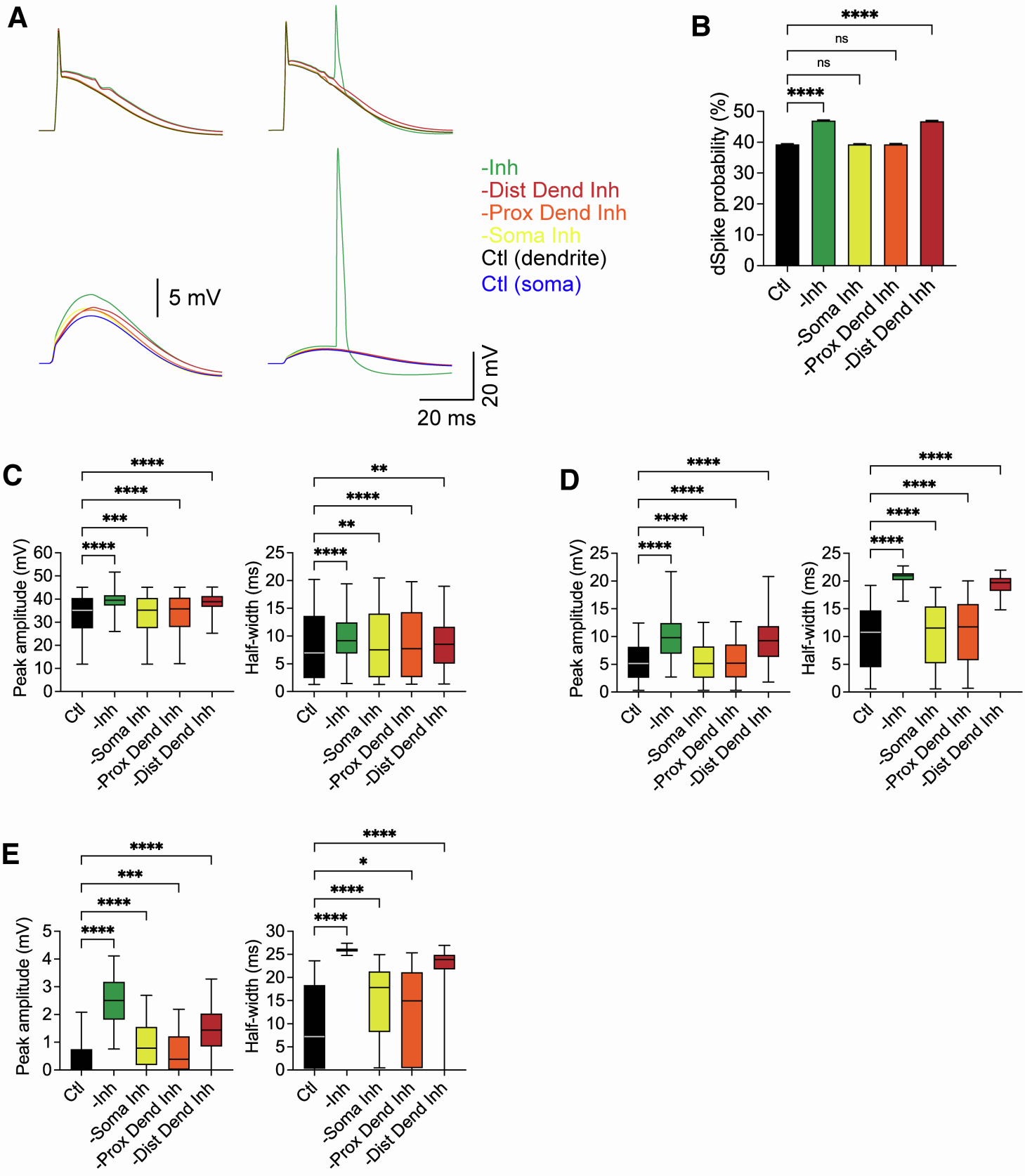
A
5 mV
20 mV
20 ms
-Inh
-Dist Dend Inh
-Prox Dend Inh
-Soma Inh
Ctl (dendrite)
Ctl (soma)
B
dSpike probability (%)
****
ns
ns
****
Ctl
-Inh
-Soma Inh
-Prox Dend Inh
-Dist Dend Inh
C
Peak amplitude (mV)
Half-width (ms)
D
Peak amplitude (mV)
Half-width (ms)
E
Peak amplitude (mV)
Half-width (ms)

Figure S12

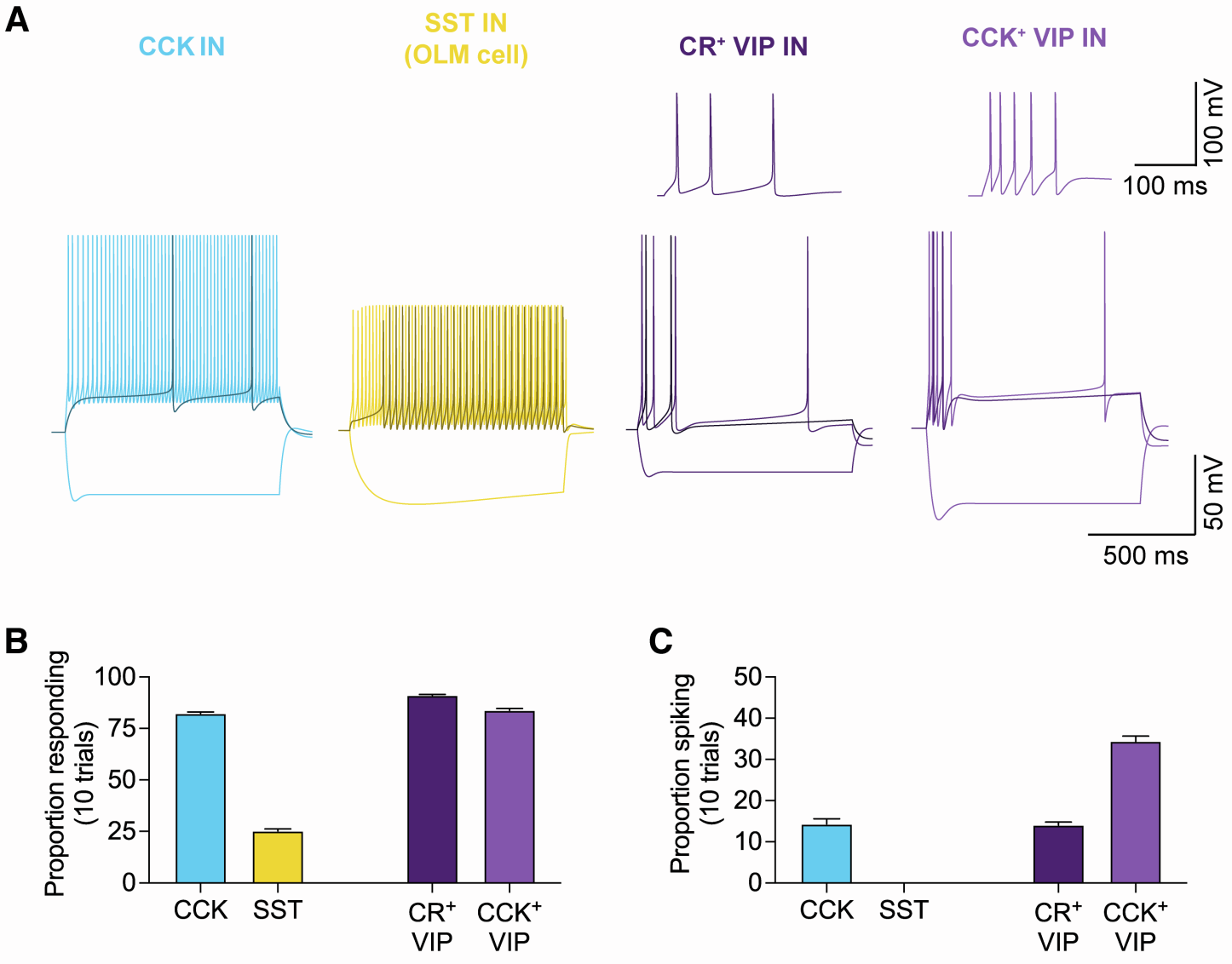
A
CCK IN
SST IN
(OLM cell)
CR+ VIP IN
CCK+ VIP IN
100 mV
100 ms
50 mV
500 ms
B
Proportion responding
(10 trials)
100
75
50
25
0
CCK
SST
CR+
VIP
CCK+
VIP
C
Proportion spiking
(10 trials)
50
40
30
20
10
0
CCK
SST
CR+
VIP
CCK+
VIP

Figure S13

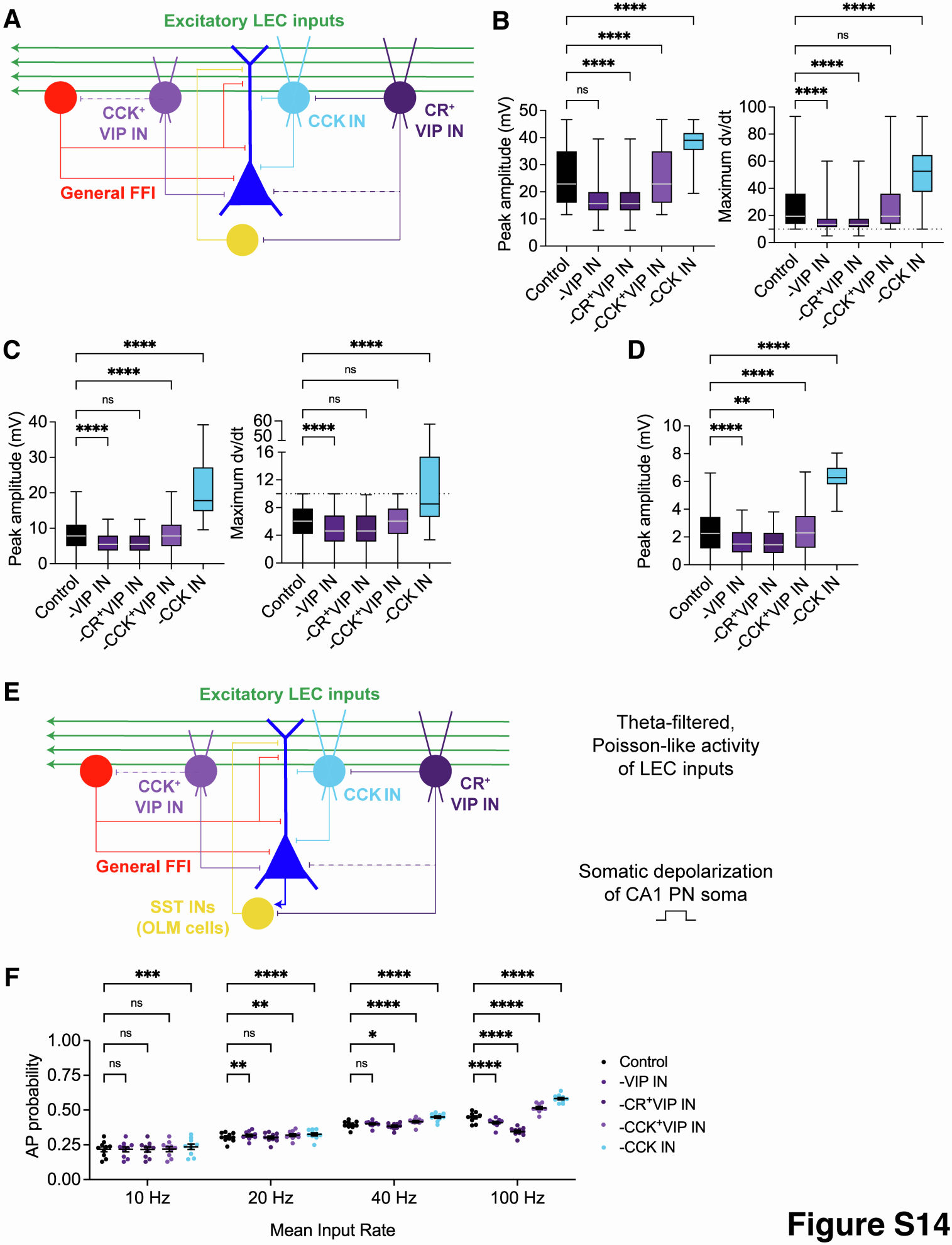
A
Excitatory LEC inputs
CCK+ VIP IN
CCK IN
CR+ VIP IN
General FFI
B
Peak amplitude (mV)
Maximum dv/dt
Control
-VIP IN
-CR+VIP IN
-CCK+VIP IN
-CCK IN
C
Peak amplitude (mV)
Maximum dv/dt
D
Peak amplitude (mV)
E
Excitatory LEC inputs
CCK+ VIP IN
CCK IN
CR+ VIP IN
General FFI
SST INs (OLM cells)
Theta-filtered, Poisson-like activity of LEC inputs
Somatic depolarization of CA1 PN soma
F
AP probability
10 Hz
20 Hz
40 Hz
100 Hz
Mean Input Rate
Control
-VIP IN
-CR+VIP IN
-CCK+VIP IN
-CCK IN

Figure S14

Name of compartment	SR/SLM CCK IN		OLM IN		CCK^+ VIP IN		CR^+ VIP IN	
	d x L (μm^2) / # compartments		d x L (μm^2) / # compartments		d x L (μm^2) / # compartments		d x L (μm^2) / # compartments	
soma	10 x 20	1	10 x 25	1	10 x 20	1	10 x 20	1
radProx	4.0 x 100	2	-	-	4.0 x 50	2	4.0 x 100	2
radMed	3.0 x 100	2	-	-	3.0 x 50	2	3.0 x 100	2
radDist	2.0 x 200	2	-	-	2.0 x 100	2	2.0 x 200	2
lmM	1.5 x 100	2	-	-	1.5 x 50	2	1.5 x 100	2
Lmt	1.0 x 100	2	-	-	1.0 x 50	2	1.0 x 100	2
oriProx	2.0 x 100	2	-	-	2.0 x 50	2	2.0 x 100	2
oriMed	1.5 x 100	2	-	-	1.5 x 50	2	1.5 x 100	2
oriDist	1.0 x 100	2	-	-	1.0 x 50	2	1.0 x 100	2
dend	-	-	3.0x250	2	-	-	-	-
axon	-	-	1.5x150	1	-	-	-	-
Total		**17**		**4**		**17**		**17**

Table S1

Name of compartment	CA1 PN	
	d x L (μm^2) / # compartments	
soma	10.0 x 10	1
axon	1.0 x 150	1
radTProx	3.0 x 80	2
radTMed	2.5 x 70	2
radTdist1	2.0 x 50	1
radTdist2	1.75 x 50	1
radTdist3	1.5 x 50	1
lm_thick	0.95 x 50	2
lm_medium	0.9 x 50	2
lm_thin	0.6 x 75	4
rad_thick	1.9 x 50	2
rad_medium	1.5 x 50	2
rad_thin	0.95 x 75	4
oriprox	1.6 x 75	2
oridist	1.1 x 75	4
Total		**29**

Table S2

Mechanism	Compartment						
	Soma	Axon	radTprox	radTmed	radTdist 1	radTdist 2	radTdist 3
Leak conductance [S/cm^2]	5e-8	5e-8	5.26e-8	6.67e-8		2.85e-7	
Na^+ conductance [S/cm^2]	3.5e-2	1.5e0	1.4e-2	1.4e-2		1.4e-2	
Delayed rectifier K^+ conductance [S/cm^2]	1.4e-3	1e-1	1.74e-3	1.73e-3		1.73e-3	
Proximal A-type K^+ conductance [S/cm^2]	7.5e-3	x	1.8e-3	x		x	
Distal A-type K^+ conductance [S/cm^2]	x	x	x	2.78e-2	3.75e-2	4.73e-2	4.86e-2
M-type K^+ conductance [S/cm^2]	1.66e-2	3e-6	6e-4	6e-4		6e-4	
I_h conductance [S/cm^2]	1.5e-5	x	1.8e-5	6e-5		9e-5	
L-type Ca^{2+} conductance [S/cm^2]	7e-3	x	3.16e-6	6.32e-6	1.27e-5	1.9e-5	2.53e-5
R-type Ca^{2+} conductance [S/cm^2]	3e-3	x	3e-4	3e-4		3e-4	
T-type Ca^{2+} conductance [S/cm^2]	5e-5	x	4e-4	4e-4		4e-4	
Ca^{2+}-dependent mAHP K^+ conductance [S/cm^2]	9.075e-2	x	6.6e-3	6.6e-3		4.12e-3	
Ca^{2+}-dependent sAHP K^+ conductance [S/cm^2]	5e-4	x	5e-4	5e-4		5e-5	
Membrane capacitance c_m [µF/cm^2]	1	1	2.2	2.2		2.2	
Membrane resistance R_m [Ohm cm^2]	200,000	200,000	190,000	150,000		35,000	
Axial resistance R_a [Ohm cm]	300	300	285	270	255	225	216
$V_{half,h}$ [mV]	-90	x	-90	-90		-90	
E_L [mV]	-70	-70	-70	-70		-70	
E_{Na} [mV]	50	50	50	50		50	
E_K [mV]	-80	-80	-80	-80		-80	
E_h [mV]	-10	x	-10	-10		-10	
E_{Ca} [mV]	140	x	140	140		140	

Table S3

Mechanism	Compartment					
	Basal dendrites		Apical tuft	Oblique dendrites		
	prox	distal		thick	med	thin
Leak conductance [S/cm^2]	5.55e-7		8.3e-7	7.7e-7	8.3e-7	8.3e-7
Na^+ conductance [S/cm^2]	7e-3		1.5e-3		8.4e-3	
Delayed rectifier K^+ conductance [S/cm^2]	8.6e-4		1.9e-4		1e-3	
Proximal A-type K^+ conductance [S/cm^2]	7.5e-3		x		x	
Distal A-type K^+ conductance [S/cm^2]	x		4.86e-2		4.17e-2	
M-type K^+ conductance [S/cm^2]	6e-4		1.2e-3		1.2e-3	
I_h conductance [S/cm^2]	1.5e-5	2.25e-5	1.2e-4		6e-5	
L-type Ca^{2+} conductance [S/cm^2]	x		3.16e-6		1.26e-5	
R-type Ca^{2+} conductance [S/cm^2]	x		x		x	
T-type Ca^{2+} conductance [S/cm^2]	x		x		x	
Ca^{2+}-dependent mAHP K^+ conductance [S/cm^2]	1.65e-2		4.125e-3		4.125e-3	
Ca^{2+}-dependent sAHP K^+ conductance [S/cm^2]	5e-4		5e-5		5e-5	
Membrane capacitance c_m [µF/cm^2]	3.0		3.0		3.0	
Membrane resistance R_m [Ohm cm^2]	18,000		12,000	13,000	12,000	12,000
Axial resistance R_a [Ohm cm]	150		150		150	
$V_{half,h}$ [mV]	-81		-90		-90	
E_L [mV]	-70		-70		-70	
E_{Na} [mV]	50		50		50	
E_K [mV]	-80		-80		-80	
E_h [mV]	-10		-10		-10	
E_{Ca} [mV]	140		140		140	

Table S4

Mechanism	Compartment						
	SR/SLM CCK IN	OLM IN			CCK^+ VIP IN	CR^+ VIP IN	
		Soma	Axon	Dendrite		Soma	Dendrites
Leak conductance [S/cm^2]	3.7e-5	5e-5	2.5e-5	2.5e-5	1.8e-5	3.1e-5	3.1e-5
Na^+ conductance [S/cm^2]	2e-1	2.6e-2	3.4e-2	4.7e-2	3.4e0	3.0e-2	9e-2
Delayed rectifier K^+ conductance [S/cm^2]	1.3e-2	4.8e-2	5.1e-2	4.6e-1	2.6e-1	3.6e-3	9e-3
A-type K^+ conductance [S/cm^2]	6e-4	1.2e-2	x	7.2e-2	1.5e-4	x	x
Slowly inactivating K^+ conductance [S/cm^2]	x	x	x	x	x	6.5e-3	x
I_h conductance [S/cm^2]	2.5e-5	1.4e-5	x	1.4e-5	2.7e-5	2.0e-4	2.7e-5
L-type Ca^{2+} conductance [S/cm^2]	2.5e-5	x	x	x	7.5e-4	3.0e-4	x
N-type Ca^{2+} conductance [S/cm^2]	1.6e-6	x	x	x	1.2e-4	1.0e-3	x
Ca^{2+}-dependent mAHP K^+ conductance [S/cm^2]	7.2e-2	x	x	x	2e-3	4.5e-4	x
Ca^{2+}-dependent sAHP K^+ conductance [S/cm^2]	4e-4	x	x	x	4e-2	4.0e-3	x
Membrane capacitance c_m [$\mu F/cm^2$]	1.1		1.6		1.3	1.4	
Axial resistance R_a [Ohm cm]	100		150		100	150	
E_L [mV]	-70	-67	-67	-65	-65	-65	
E_h [mV]	-40		-32.9		-40	-40	-32.9
E_{Na} [mV]	55		50		55	55	
E_K [mV]	-85		-77		-85	-85	
E_{Ca} [mV]	130		x		130	130	x
τ_{Ca} [ms]	9		x		70	20	x

Table S5

From/to		CA1 PNs		SR/SLM CCK INs	OLM INs	CCK^+ VIP INs	CR^+ VIP INs
LEC LIII		AMPA	NMDA	AMPA	AMPA	AMPA	AMPA
	g (nS)	1.5e-3	3.7e-4	1.8e-3	1.3e-3	7.7e-4	1.2e-3
	τ_r (ms)	1.0	2.3	0.5	0.5	0.5	0.5
	τ_d (ms)	10.0	100.0	3.0	8.0	3.0	3.0
CA1 PNs		AMPA		AMPA	AMPA	AMPA	AMPA
	g (nS)	x		x	2.5e-3	x	x
	τ_r (ms)	x		x	0.5	x	x
	τ_d (ms)	x		x	8.0	x	x
SR/SLM CCK INs		$GABA_A$	$GABA_B$	$GABA_A$	$GABA_A$	$GABA_A$	$GABA_A$
	g (nS)	1.5e-3	1.5e-3	x	x	x	x
	τ_r (ms)	1.0	1.0	x	x	x	x
	τ_d(ms)	11.0	50.0	x	x	x	x
OLM INs		$GABA_A$	$GABA_B$	$GABA_A$	$GABA_A$	$GABA_A$	$GABA_A$
	g (nS)	1.5e-3	1.5e-3	x	x	x	x
	τ_r (ms)	1.0	1.0	x	x	x	x
	τ_d (ms)	11.0	50.0	x	x	x	x
CCK^+ VIP INs		$GABA_A$		$GABA_A$	$GABA_A$	$GABA_A$	$GABA_A$
	g (nS)	3.8e-4		x	x	x	x
	τ_r (ms)	0.3		x	x	x	x
	τ_d (ms)	8.0		x	x	x	x
CR^+ VIP INs		$GABA_A$		$GABA_A$	$GABA_A$	$GABA_A$	$GABA_A$
	g (nS)	x		1.9e-1	1.9e-2	x	x
	τ_r (ms)	x		0.73	1.3	x	x
	τ_d (ms)	x		5.1	9.0	x	x

Table S6

Supplemental Materials and Text

Figure S1. LEC infection confirmed by confocal imaging and local recordings. Related to Figure 1.
(A) Cartoon illustrating the extent of viral infection in LEC with AAV-CaMKII-ChR2-eYFP. Generated from 25 representative high-resolution confocal images of patched brain slices containing LEC.
(B) Example confocal image of LEC expressing ChR2-eYFP (green).
(C) Positive control: ChR2 function in an infected LEC neuron. Top: Time-locked responses recorded in cell-attached mode in response to a maximum strength 10 Hz photostimulation train. Bottom: Large, excitatory photocurrent recorded in whole-cell configuration in response to 500 ms photostimulation. Enlarged photocurrent shown to the left. Photostimulation done over LEC.
(D) Negative control: Lack of viral infection in a non-infected CA1 PN. Same protocols used as in (C). Photostimulation done over CA1.
(E) Cartoon illustrating the distribution of somatic (blue) and dendritic (black) recordings along the proximal-distal and radial axes of hippocampal area CA1. Dendrites that exhibited LEC-driven dSpikes are represented by asterisks.

Figure S2. Properties of CA1 PN compartments and monosynaptic drive from glutamatergic LEC inputs. Related to Figure 1.
(A) Additional examples of electrophysiological properties of CA1 PN dendrites. Left: 800 pA, 500 pA, and -350 pA dendritic current injection. Right: 800 pA, 200 pA, and -275 pA dendritic current injection. The dendritic membrane potential was maintained at -70 mV.
(B) Summary firing properties (left) and sag (right) in CA1 PN dendrites. Individual data are shown in gray. Mean ± SEM are shown in black. n = 14 dendrites.
(C) Resting membrane potential of CA1 PN distal dendrites. Mean ± SEM: -62.73 ± 0.92 mV. n = 17 dendrites.
(D) Input resistance of CA1 PN distal dendrites. Mean ± SEM: 287.8 ± 39.1 MΩ. n = 17 dendrites.
(E) Additional examples of electrophysiological properties of CA1 PN somata. Left: 275 pA, 50 pA, and -250 pA somatic current injection. Right: 225 pA, 125 pA, and -300 pA somatic current injection. The somatic membrane potential was held at -70 mV.
(F) Summary firing properties (left) and sag (right) in CA1 PN somata. Individual data are shown in light blue. Mean ± SEM are shown in blue. n = 43 somata.
(G) Resting membrane potential of CA1 PN somata. Mean ± SEM: -68.16 ± 0.32 mV, n = 51 somata.
(H) Input resistance of CA1 PN somata. Mean ± SEM: 142.4 ± 6.82 MΩ, n = 54 somata.
(I) Example LEC-driven response in a CA1 PN soma recorded in control conditions (blue) and after application of TTX and 4-AP (dark blue), respectively.

Figure S3. Derivative and phase plots of LEC-driven responses in CA1 PN distal dendrites. Related to Figure 2.
(A) Example LEC-driven post-synaptic responses, as shown in Figure 2A. Ordered by amplitude.
(B) Corresponding LEC-driven responses (top), derivative traces (middle), and phase plots (bottom) of the example dendrites, demonstrating the visible differences between LEC-driven dPSPs (shades of yellow, left) and LEC-driven dSpikes (shades of blue, right).

Figure S4. Comparisons of various LEC-driven responses in CA1 PNs. Related to Figures 1 and 2.

(A-G) Subthreshold versus suprathreshold LEC-driven responses in CA1 PN distal dendrites. Resting membrane potential ($p = 0.1806$), recording location ($p = 0.8798$), response amplitude ($p = 0.0264$), time of peak ($p = 0.1695$), rise time ($p = 0.2112$), half-width ($p = 0.0011$), maximum dV/dt ($p = 0.0097$). Unpaired t-test with Welch's correction. n = 14 dPSPs and n = 5 dSpikes.

(H) Relationship between the recording location, amplitude, and maximum dV/dt value of the LEC-driven dendritic responses.

(I-O) Subthreshold LEC-driven PSPs in the dendrite versus soma.

(I) All light-evoked PSPs recorded in CA1 PN dendrites (left) and somata (middle). Individual data shown in gray. Average dendritic PSPs (black) and somatic PSPs (blue) are shown overlaid (left, middle) and directly compared (right).

(J-O) Compartment-specific differences in LEC-driven PSPs in the dendrite ("D") versus soma ("S"). Peak amplitude ($p < 0.0001$), time of peak ($p < 0.0001$), rise time ($p < 0.0001$), half-width ($p < 0.0001$), hyperpolarization amplitude ($p = 0.0927$), input resistance ($p = 0.0001$). Mann Whitney test. n = 14 dendritic PSPs and n = 52 somatic PSPs.

Figure S5. Short-term plasticity dynamics and summation of LEC inputs onto CA1 PN somata and dendrites. Related to Figures 1 and 2.

(A-E) Short-term plasticity dynamics measured in CA1 PN somata. n = 5, 5, 9, 9, and 15 somata, tested with 1, 2, 4, 8, and 10 Hz photostimulation, respectively.

(A) Experimental strategy. Low strength (2-3% maximum) photostimulation trains were given at physiological frequencies (1-10 Hz). Photostimulation done over SLM.

(B) Example LEC-driven responses in CA1 PN somata.

(C) Paired pulse ratios (PPR) at various frequencies.

(D-E) First (D) and last (E) PPR measured in the experiments described in (A). One sample t-test comparing mean PPR to hypothetical mean = 1.

(F-K) Postsynaptic summation measured in CA1 PN somata. n = 13, 14, 14, and 13 somata, tested with 2, 4, 8, and 10 Hz photostimulation, respectively.

(F) Experimental strategy. Maximum strength (100%) photostimulation trains were given at physiological frequencies (2-10 Hz). Photostimulation done over SLM.

(G) Example LEC-driven responses in CA1 PN somata.

(H) Amplitude ratios at various frequencies.

(I-J) First (I) and last (J) amplitude ratios measured in the experiments described in (F). One sample t-test comparing mean ratio to hypothetical mean = 1.

(K) Summary graph of peak response amplitudes, illustrating the lack of LEC-driven APs in CA1 PN somata. Individual data shown in faded blues. Average data shown in full opacity blues.

(L-O) Post-synaptic responses after repeated LEC input activity measured in CA1 PN distal dendrites. n = 5 dendrites.

(L) Experimental strategy. Maximum strength photostimulation trains were given at 8 Hz to measure the dendritic post-synaptic responses after repeated photostimulation of LEC inputs. Photostimulation was done over SLM.

(M) Example LEC-driven dendritic response in a CA1 PN dendrite. Squares indicate dendritic spikes.

(N) First and last amplitude ratios measured in the experiment described in (L). One sample t-test comparing mean ratio to hypothetical mean = 1.

(O) Summary graph of the spike probability in CA1 PN somata (blue) and dendrites (black) during single, 2 ms (circle) or maximum strength, 8 Hz (diamond) photostimulation. AP probability was calculated for soma, whereas dSpike probability was calculated for dendrites. n = 17 dendrites tested with single photostimulation; 5 dendrites tested with 8 Hz photostimulation; 50 somata tested with single photostimulation; and 19 somata tested with 8 Hz photostimulation.
*$p < 0.05$, ***$p < 0.001$.

Figure S6. Interneuron subgroups in hippocampal area CA1, as defined by soma location. Related to Figures 4 and 6.
(A) Left: Cartoon illustrating the distribution of recorded CA1 INs along the proximal-distal and radial axes of hippocampal area CA1. Right: Distribution of candidate interneuron populations ans subpopulations in hippocampal area CA1, based on the quantification of tdTomato-labeled cells in CA1 layers, scaled by imaging volume.
(B-C) Interneurons categorized by their soma location in CA1.
(B) Percent of INs that responded to LEC axon photostimulation. Total n = 20 SP VIP INs, 15 SLM VIP INs, 9 SP CCK INs, 14 SR/SLM CCK INs, 10 SO SST INs, 4 SP SST INs; 7 SP CR^+ VIP INs, 16 SR/SLM CR^+ VIP INs, 9 SP CCK^+ VIP INs, 16 SR/SLM CCK^+ VIP INs.
(C) Percent of LEC-driven INs that exhibited APs. n = 18 SP VIP INs, 15 SLM VIP INs, 5 SP CCK INs, 14 SR/SLM CCK INs, 1 SO SST IN, 3 SP SST INs; 6 SP CR^+ VIP INs, 15 SR/SLM CR^+ VIP INs, 6 SP CCK^+ VIP INs, 15 SR/SLM CCK^+ VIP INs.

Figure S7. Validation of optogenetic silencing in local Jaws-expressing VIP INs. Related to Figure 5.
(A) Injection strategy. Same as in Figure 5A.
(B) Confocal images of hippocampal area CA1 of a VIP-Cre/Ai14 mouse, demonstrating the infection of $tdTomato^+$ VIP INs (red) with Jaws-GFP (green), spanning various CA1 layers (white insets, right).
(C) Experimental strategy. Targeted recordings and optogenetic silencing of local VIP INs in area CA1 (yellow-filled purple neurons) to validate Jaws function. $Jaws^+$ VIP INs were photostimulated with 625 nm light (maximum strength) for 10-1000 ms.
(D) Hyperpolarization amplitude recorded from $Jaws^+$ VIP INs upon photostimulation with 625 nm light. Mean ± SEM shown in black. n = 31 VIP INs.
(E) Positive control: 625 nm light can effectively silence action potential firing in $Jaws^+$ VIP INs.
(F) Spike frequency in $Jaws^+$ VIP INs during positive current injection before (purple) and during (red) photostimulation with 625 nm light. Individual data shown in faded colors. Averages shown in full opacity colors. n = 19 VIP INs.
(G) Example hyperpolarization in a $Jaws^+$ VIP IN during photostimulation with different durations of 625 nm light (10 ms increments, up to 100 ms).
(H) Hyperpolarization amplitude during photostimulation with different durations of 625 nm light. Individual data shown in gray. Mean ± SEM amplitude shown in red.
(I) Hyperpolarization amplitude, normalized to the maximum hyperpolarization, as recorded in (H). Mean normalized amplitude shown in black. Dotted vertical lines indicate where the normalized amplitude is at its maximum (50-60 ms).
(J) Representative confocal images demonstrating adequate (left) or poor (right) Jaws expression in CA1 VIP INs. Data collected from brain slices with poor or no Jaws expression were excluded from further analyses in this study.

(K) Relationship between Jaws expression and the effect of VIP silencing on LEC-driven dendritic (top) and somatic (bottom) responses. Linear regression lines and R^2 values indicated. The slope is significantly non-zero for dendritic data ($p = 0.0371$), but not for somatic data ($p = 0.6088$).

Figure S8. Effect of VIP IN silencing on LEC-driven dendritic and somatic responses in CA1 PNs. Related to Figure 5.
(A) Additional example traces of subthreshold LEC-driven dPSPs in control (black) and –VIP INs (red) conditions. Dotted lines indicate the peak amplitude of the dPSP.
(B) Subthreshold LEC-driven dPSP parameters before and after VIP IN silencing, average values. Paired t-test. n = 18 dendrites, 18 slices, 13 mice.
(C) Additional example traces of suprathreshold LEC-driven dSpikes in control (black) and -VIP IN (red) conditions.
(D) Suprathreshold LEC-driven dSpike parameters before and after VIP IN silencing, average values. Paired t-test. n = 5 dendrites, 5 slices, 4 mice.
(E) Example traces of LEC-driven somatic PSPs in control (blue) and –VIP INs (red) conditions. Blue and red dotted lines indicate the peak amplitude of the PSP in control and -VIP INs conditions, respectively.
(F) LEC-driven somatic PSP parameters before and after VIP IN silencing. Paired t-test. n = 7 CA1 PN somata, 5 slices, 3 mice.
*$p < 0.05$, **$p < 0.01$.

Figure S9. Attempts to selectively silence CCK INs in area CA1. Related to Figure 5.
(A-F) Strategy #1: AAV2.8-nEF-Con/Fon-iC++-eYFP virus in CCK-Cre/Dlx-Flp/Ai65 mice.
(A) Confocal image of a CCK-Cre/Dlx-Flp/Ai65 mouse injected into area CA1 with AAV2.8-nEF-Con/Fon-iC++-eYFP, incubated for 19 days. Bottom: iC++-expressing ($TdTomato^+$/$eYFP^+$) CCK INs in SLM (left) and SP (right).
(B) Example iC++-expressing CCK IN exhibiting depolarization and AP firing in response to 470 nm photostimulation.
(C) Response amplitudes of CCK INs tested 470 nm light only (left, n = 11), tested with 470 nm and 625 nm (middle, n = 7), and tested with all possible wavelengths (right, n = 4). Different wavelengths of light were shined separately.
(D) Infected CCK IN exhibiting AP firing in cell-attached mode in response to 470 nm photostimulation at 10 Hz.
(E) Response amplitudes of CA1 PNs tested 470 nm and 625 nm photostimulation (n = 4). Cells were blind-patched.
(F) Percent of patched cells that responded to 470 nm light. Total n = 11 CCK INs and 4 CA1 PNs. All photostimulated CCK INs exhibited depolarization, rather than hyperpolarization (silencing).
(G-J) Strategy #2: Custom-made AAV2.9-hDlx-Flex-Jaws-TdTomato virus in CCK-Cre mice.
(G) Confocal image of a CCK-Cre mouse injected into area CA1 with AAV2.9-hDlx-Flex-Jaws-TdTomato, incubated for 2 weeks (left) and 6 weeks (right). Inset: infected neurons in various CA1 layers (middle).
(H) Representative light-evoked response in a Jaws-$TdTomato^+$ CCK IN in response to 625 nm photostimulation, 6 weeks after viral injection.
(I) Hyperpolarization amplitudes of all tested Jaws-$TdTomato^+$ CCK INs sampled, across various viral incubation periods.

(J) Firing properties of Jaws-TdTomato$^+$ CCK INs in control (black) and attempted silencing (red) conditions, 6 weeks after viral injection. Individual data shown in faded colors. Average data shown in full opacity colors. n = 8 CCK INs.
(K-P) Strategy #3: AAV2.5-CAG-Flex-Jaws-GFP virus in CCK-Cre mice.
(K) Confocal image of a CCK-Cre mouse injected into area CA1 with AAV2.5-CAG-Flex-Jaws-GFP (same virus as in Figure 5), incubated for 19 days.
(L) Example traces from a CCK IN, CA1 PN soma, and CA1 PN dendrite, demonstrating appropriate (CCK IN) or off-target (CA1 PN soma and dendrite) hyperpolarization in response to 625 nm photostimulation. CCK INs were patched in a targeted manner, based on GFP expression. CA1 PN somata and dendrites were blind-patched.
(M) Percent of patched cells that exhibited hyperpolarization in response to 625 nm photostimulation. Total n = 5 CCK INs, 22 CA1 PN somata, and 11 CA1 PN dendrites. CA1 PN somatic patch data is pooled. CA1 PN dendritic patch data is pooled.
(N) Hyperpolarization amplitudes of all tested CCK INs, CA1 PN somata, and CA1 PN dendrites, tested across various viral injection dilutions and incubation times. Standard protocol: non-diluted virus, 15-18 day viral incubation.
(O-P) Attempted experiment: effect of CCK IN silencing on LEC-driven dendritic responses in CA1 PNs.
(O) Confocal image of a CCK-Cre mouse, co-injected with AAV2.5-CAG-Flex-Jaws-GFP into CA1 and AAV2.9-CaMKII-ChR2-eYFP into LEC. Patched (and infected) CA1 PN was filled with biocytin and counterstained with streptavidin 647 (yellow). Both viruses are visible in green.
(P) LEC-driven response in the CA1 PN dendrite from (O), tested under control (black) and 625 nm photostimulation (red) conditions. Jaws virus and ChR2 virus were incubated for 9 days.

Figure S10. Local VIP IN subtypes exhibit disinhibitory and inhibitory functions. Related to Figure 6.
(A) Experimental strategy. Photostimulation (blue) of CR$^+$ VIP INs or CCK$^+$ VIP INs (light green) and somatic voltage clamp recordings from putative PNs (blue) and INs (red) in hippocampal area CA1. Neurons were held at +10 mV to record IPSCs.
(B) Proportion of recorded CA1 PNs and layer-specific INs that were inhibited by CR$^+$ VIP INs. Total n = 16 PNs, 11 SO INs, 9 SR INs, and 9 SLM INs.
(C) CR$^+$ VIP IN-driven IPSCs from responding CA1 PNs and layer-specific INs. Traces from individual neurons shown in gray. Average IPSC trace shown in blue (PN) or red (INs). Proportion of inhibited cells noted above the traces.
(D) Example morphological reconstructions of neurons inhibited by CR$^+$ VIP INs. Left to right (top): perforant path-associated cell, putative CCK$^+$ VIP IN basket cell, Schaffer collateral-associated cell. Left to right (bottom): CA1 PN, horizontal basket or axo-axonic cell, and OLM cell. Soma and dendrites shown in black. Axon shown in blue. Scale bars 100 μm.
(E) Proportion of recorded CA1 PNs and layer-specific INs that were inhibited by CCK$^+$ VIP INs. Total n = 23 PNs, 11 SO INs, 11 SR INs, and 9 SLM INs.
(F) CCK$^+$ VIP IN-driven IPSCs from responding CA1 PNs and layer-specific INs. Traces from individual neurons shown in gray. Average IPSC trace shown in blue (PN) or red (INs). Proportion of inhibited cells noted above the traces.
(G) Example morphological reconstructions of neurons inhibited by CCK$^+$ VIP INs. Left to right: Schaffer collateral-associated cell, two CA1 PNs, and OLM cell. Soma and dendrites shown in black. Axon shown in blue. Scale bars 100 μm.

Figure S11. Model validation: CA1 PN intrinsic properties and dSpike generation. Related to Figure 7.
(A-C) Top: simulated dendritic recordings (300 μm from the soma, black). Bottom: simulated somatic recordings (blue).
(A) Example electrophysiological properties. Firing properties and sag were measured in response to simulated depolarizing or hyperpolarizing current injections, respectively. The compartment membrane potential was held at -70 mV.
(B-C) Example firing properties (B) and sag (C).
(D) Example dendritic spikes generated by the computational model.
(E) Box and whisker plots comparing simulated subthreshold and suprathreshold LEC-driven responses. Plus sign represents the mean. Mann Whitney test, n = 200 dendritic PSPs and 200 dendritic spikes. *$p < 0.05$, ****$p < 0.0001$.

Figure S12. Simulation: compartment-specific inhibition blockade. Related to Figure 7.
(A) Example LEC-driven responses in the model CA1 PN before and after compartment-specific inhibition removal. Top: dendritic recordings. Bottom: somatic recordings. Control dendritic and somatic recordings shown in black and blue, respectively. Complete inhibition removal shown in green. Distal dendritic, proximal dendritic, and somatic inhibition removal shown in red, orange, and yellow, respectively.
(B) Dendritic spike probability after removal of compartment-specific inhibition. Tukey's multiple comparisons test. n = 50 x 1000 trials.
(C) Box and whisker plots of LEC-driven dSpike amplitude (left) and half-width (right) recorded in control conditions and upon removal of compartment-specific inhibition.
(D) Box and whisker plots of LEC-driven dPSP amplitude (left) and half-width (right) recorded in control conditions and upon removal of compartment-specific inhibition.
(E) Box and whisker plots of LEC-driven somatic PSP amplitude (left) and half-width (right) recorded in control conditions and upon removal of compartment-specific inhibition.
(C-E) Dunn's multiple comparisons test. n = 100 trials.
*$p < 0.05$, **$p < 0.01$, ***$p < 0.001$, ****$p < 0.0001$.

Figure S13. Model validation: LEC-driven GABAergic INs in CA1. Related to Figure 7.
(A) Example electrophysiological properties of the INs, generated by the model. Firing properties and sag were measured in response to simulated depolarizing or hyperpolarizing current injections into the IN soma, respectively. CCK IN: 350, 100, and -300, SST IN: 250, 100, and -200, CR^+ VIP IN: 150, 75, and -200, and CCK^+ VIP IN: 250, 100, and -200 pA current injected. The trace generated from the middle current injection is shown in a darker color. The traces above the VIP INs zoom into the APs generated by the highest depolarizing current injection. The IN membrane potential was held at -70 mV.
(B) Percent of INs that responded to excitatory LEC inputs in the model.
(C) Percent of responding INs that exhibited LEC-driven APs in the model.
(B-C) Calculated from 10 runs of the model, with 200 trials per run.

Figure S14. Simulation: Effect of IN deletion on LEC-driven dendritic activity and somatic output in a CA1 PN. Related to Figure 7.
(A) Model circuit schematic, same as in Figure 7C.

(B) Box and whisker plots of LEC-driven dSpike amplitude (left) and maximum dV/dt (right) under control and IN deletion conditions. Simulated LEC-driven dendritic responses were classified as dSpikes if the maximum dV/dt > 10 mV/ms in control conditions.
(C) Box and whisker plots of LEC-driven dPSP amplitude (left) and maximum dV/dt (right) under control and IN deletion conditions. Simulated LEC-driven dendritic responses were classified as dPSPs if the maximum dV/dt < 10 mV/ms in control conditions.
(D) Box and whisker plots of LEC-driven somatic response amplitude under control and IN deletion conditions.
(B-D) Dunn's multiple comparison's test. n = 200 trials.
(E) Model circuit schematic (left) and description of activity patterns (right). The model was calibrated to produce LEC-driven APs in the CA1 PN soma through a combination of somatic depolarization and theta-filtered Poisson-like activity of excitatory LEC inputs at various frequencies (10-100 Hz). OLM INs were recruited within the microcircuit in the recalibrated model because the CA1 PN exhibited APs.
(F) LEC-driven action potential probability of the model CA1 PN under control and IN deletion conditions. Tukey's multiple comparison test. n = 10 x 1000 trials.
*p < 0.05, **p < 0.01, ***p < 0.001, ****p < 0.0001.

Table S1. **Morphological properties of the model GABAergic interneurons. Related to Figure 7.** d and L denote the diameter and length of the compartments, respectively.

Table S2. Morphological properties of the model CA1 PN. Related to Figure 7.
Prefix 'radT' in compartments correspond to the apical trunk, 'rad' to oblique dendrites, 'lm' to apical tuft, and prefix 'ori' to basal dendrites, respectively. d and L denote the diameter and length of the compartment.

Table S3. Passive parameters and active ionic conductances for somatic, axonal, and apical dendritic trunk compartments of the model CA1 PN. Related to Figure 7.

Table S4. Passive parameters and active ionic conductances for basal (SO), apical tuft (SLM), and oblique (SR) dendrites of the model CA1 PN. Related to Figure 7.

Table S5. Passive parameters and active ionic conductances for all interneurons and their compartments when applicable. Related to Figure 7.

Table S6. Synaptic properties of the canonical circuitry. Related to Figure 7.